

This is the submitted version of the following article

Libor Červenka, Anna Stępień, Michaela Frühbauerová, Helena Velichová, Mariusz Witczak (2019). Thermodynamic properties and glass transition temperature of roasted and unroasted carob (*Ceratonia siliqua* L.) powder. *Food Chemistry*. DOI: 10.1016/j.foodchem.2019.125208

This submitted version is available from URI <https://hdl.handle.net/10195/74882>

Publisher's version is available from:

<https://www.sciencedirect.com/science/article/pii/S0308814619313159?via%3Dihub>

Manuscript Number:

Title: Thermodynamic properties and glass transition temperature of roasted and unroasted carob (*Ceratonia siliqua* L.) powder

Article Type: VSI: Water in Food

Keywords: isotherm; enthalpy; entropy; spreading pressure; compensation theory

Corresponding Author: Mr. Libor Cervenka, Ph.D.

Corresponding Author's Institution: University of Pardubice

First Author: Libor Cervenka, Ph.D.

Order of Authors: Libor Cervenka, Ph.D.; Anna Stepien; Michaela Fruhbauerova; Helena Velichova; Mariusz Witczak

Abstract: Moisture adsorption isotherms of unroasted and roasted carob powder (*Ceratonia siliqua* L.) at 15, 25, and 40 °C were determined by the static gravimetric method over the wide range of water activity from 0.06 to 0.90. GAB model fitted well the experimental adsorption data showing sigmoid shape curves for both samples. Claussius-Clapeyron equation showed that the adsorbed moisture is strongly bound to the surface of unroasted carob powder in low moisture content than that in roasted sample. The variation of the net integral enthalpy and entropy with the moisture content exhibited maximal and minimal values for unroasted carob powder at low moisture content, respectively. Gradual decrease in enthalpy and increase in entropy were observed for roasted carob powder. Combining the glass transition temperature lines with adsorption isotherms, it was found that roasted carob powder is stable up to 43 aw in comparison with unroasted carob powder (up to 38 aw).



Univerzita
Pardubice
Fakulta
chemicko-technologická

Editorial office of
Food Chemistry

Pardubice 19.02. 2019

Dear editor,

We are sending you a manuscript entitled “*Thermodynamic properties and glass transition temperature of unroasted and roasted carob (Ceratonia siliqua L.) powder*”. Carob powder is a valuable product with high content of dietary fibre and polyphenolic substances. Carob powder/flour is usually sold as such (after milling dried pods) or roasted in order to promote cocoa-like aroma and develop product with higher antioxidants content, as was mentioned in Introduction. We prepared manuscript with scientific data which were partly presented in The 10th International Conference on Water in Food. We have focused on the thermodynamic analysis of carob powder (unroasted and roasted) as a part of our research. To the best of our knowledge, there is no data available on that topic in scientific journal.

We hope that you will find this manuscript worth to the broader audience and suitable for publication in *Food Chemistry VSI: Water in Food*) as an **original research article**. The manuscript contains **4641** words, **2** tables, **4** figures and **37** references. In addition, supplementary materials were also prepared.

Yours sincerely

Assoc. prof. Libor Cervenka, Ph.D.
Department of Analytical Chemistry
Faculty of Chemical Technology
University of Pardubice
Tel.: +420 466 037 718
Fax: +420 466 037 068
e-mail libor.cervenka@upce.cz

*Highlights (for review)

- GAB isotherms successfully described the experimental moisture content data
- Strongly bound water molecules in unroasted carob powder were observed
- Different integral thermodynamic properties were determined
- Roasted carob powder exhibited better stability

Libor ČERVENKA^{1*}, Anna STEPIEŃ², Michaela FRÜHBAUEROVÁ¹, Helena VELICHOVÁ³, Mariusz WITCZAK²

Thermodynamic properties and glass transition temperature of roasted and unroasted carob (*Ceratonia siliqua* L.) powder

¹Department of Analytical Chemistry, Faculty of Chemical Technology, University of Pardubice, Studentská 573, 53210 Pardubice, Czechia

² Department of Engineering and Machinery for Food Industry, Faculty of Food Technology, University of Agriculture, Balicka 122 Street., 30-149 Krakow, Poland

³ Department of Food Analysis and Chemistry, Faculty of Technology, Tomáš Baťa University in Zlín, Vavrečkova 275, 760 01 Zlín, Czechia

* corresponding author Libor Červenka; e-mail: libor.cervenka@upce.cz; tel.: +420466037718, fax:+420466037068

Anna STEPIEŃ, anna.stepien@urk.edu.pl

Michaela FRÜHBAUEROVÁ, fruhbauerova.michaela@gmail.com

Helena VELICHOVÁ, velichova@ft.utb.cz

Mariusz WITCZAK, rrwitcza@cyf-kr.edu.pl

1 1. Introduction

2

3 Carob powder is the product of the fruit of *Ceratonia siliqua L.* The powder is usually
4 prepared from mature, dried carob pod (without seed) after milling to desired particle size.

5 Carob powder is a good source of sucrose and other simple sugars (maltose, mannose),
6 unsaturated fatty acids and minerals such as calcium, potassium and iron (Ayaz et al., 2009).

7 High content of dietary fibre is the most important parameter, which makes the carob powder
8 applicable in various food products such as pasta or bread (Biernacka, Dziki, Gawlik-Dziki,

9 Rozylo, & Siastala, 2017; Turfani, Narducci, Durazzo, Galli, & Carcea, 2017). Carob powder

10 is also used as a replacer of cocoa in cocoa- and chocolate-based products decreasing the

11 content of caffeine and theobromine but keeps the cocoa-like aroma, particularly when

12 roasting (Loullis & Pinakoulaki, 2018). In addition, carob powder is the rich source of

13 polyphenolic substances exhibited promising effects on the human health acting such as

14 antioxidant, antibacterial, anti-inflammatory, and anti-diabetic agents (Rtibi et al., 2017).

15 The knowledge of moisture sorption behaviour of food matrix is crucial to select appropriate

16 packaging material or storage condition. Several studies have reported about the moisture

17 adsorption of various plant-based powders such as elecampe and burdock root powders

18 (Cervenka, Kubinova, Juszczak, & Witczak, 2012), chironji kernels (Sahu et al., 2018), coffee

19 (Baptestini, Correa, de Oliveira, Cecon, & Soares, 2017; de Oliveira et al., 2017), sesame seed

20 (Kaya & Kahyaoglu, 2006) or wheat and chestnut flour (Moreira, Chenlo, Torres, & Prieto,

21 2010). Equilibrium relationship of the moisture content and water activity at the constant

22 temperature has to be determine for calculation of various properties of sorbed water and

23 thermodynamic characteristics of sorption process. There are many empirical equations

24 proposed for describing the moisture adsorption of food material (Al-Muhtaseb, McMinn, &

25 Magee, 2002) with Guggenheim-Anderson-de Boer's (GAB) equation as the most frequent

26 used mathematical description of experimental moisture sorption data, which can be applied
27 in the wide range of water activities. GAB equation is also preferred as it provides monolayer
28 moisture content, a key parameter corresponding to the stability of the food material.
29 The thermodynamic analysis of equilibrium moisture sorption data provides a closer insight
30 into the microstructure of food material and describes the interaction in water-substrate
31 interface. The isosteric heat of sorption, differential entropy, integral enthalpy and entropy
32 describe the behaviour of water and the energy requirements of heat and mass transfer in
33 biological material (Cervenka, Hlouskova, & Zabcikova 2015; McMinn, McKee, Ronald, &
34 Magee, 2007; de Oliveira et al., 2017; Polatoglu, Bese, Kaya, & Aktas, 2011).
35 Despite the fact that water activity is an important parameter describing available water in
36 biological material, it is not sufficient to describe the secondary processes of change-in-state
37 in foodstuffs. Some deteriorative changes in food such as stickiness, caking, crystallization
38 and structural collapse are related to its rubbery state. Hence, water activity has been often
39 combine with glass transition temperature (T_g) to provide an integrated approach to study the
40 role of water in foods (Tonon et al., 2009). The glass transition is a thermodynamic second-
41 order phase transition, from glassy to rubbery state, which is related with the change in the
42 heat capacity of the material that occurs over temperature range. The main difference between
43 the two states is related to molecular mobility: very low in glassy and higher in rubbery state.
44 In general, the glassy state can be considered as a more stable in the shelf life of foodstuff
45 than glassy form (Mosquera, Moraga, & Martinez-Navarrete, 2012). The glass transition
46 temperatures of biological materials depend mainly on the quantity of water, chemical
47 composition and molecular weight of the solutes present in material (Rahman, 2006).
48 Although carob powder and flour are used in various formulas, there is no data about moisture
49 sorption and thermodynamic properties in the literature. Therefore, the aim of this study is to
50 determine the moisture adsorption behaviour of unroasted and roasted carob powder, to

51 elucidate their thermodynamic properties and glass transition phenomena in relation to their
52 storage stability. The roasting process changes the thermodynamic of moisture adsorption is
53 the hypothesis which is evaluated in this study.

54

55 2. Materials and methods

56 2.1 Sample preparation

57 Dry carob pods (*Ceratonia siliqua* L.) without seed were purchased in local supplier. Pods
58 were milled using knife mill Grindomix GM 200 (Retsch[®], Haan, Germany) to obtain
59 powder. The powder was passed through analytical sieve to get particles smaller than 600 μm ,
60 which were subsequently used for further experiment. The roasting condition was chosen with
61 respect to the low content of toxic Maillard reaction products as was described by (Cepo et
62 al., 2014), i.e. the carob powder was heated in drying oven at 130 °C for 30 min in 0.5 cm
63 layer's thickness. Both roasted and unroasted carob powder samples were stored in evacuated
64 plastic bag at room temperature until used.

65

66 2.3 Chemical analysis

67 Crude fat (920.85), crude protein (920.87), reducing sugars (939.03), total dietary fibre
68 (985.29) and ash content (923.03) were determined according to AOAC official methods
69 (AOAC, 2007).

70

71 2.4 Moisture adsorption study

72 Prior the moisture adsorption study, carob powder was carefully dehydrated in closed
73 desiccator with freshly dried silica gel until the weight constancy. Static gravimetric method
74 was applied to examine equilibrium moisture content (EMC; $\text{g H}_2\text{O g}^{-1}$ dry basis, db) at
75 particular water activity level. Briefly, salt slurries (LiBr, LiCl, CH_3COOK , MgCl_2 , K_2CO_3 ,

76 Mg(NO₃)₂, NaBr, CoCl₂, KI, NaCl, KCl, K₂SO₄) were prepared to induce water activity level
77 in the range from 0.058 to 0.980 as was described by (Greenspan, 1977). Approximately 1.0 g
78 of sample was placed above salt slurry in desiccator and equilibrated at 15, 25, and 40 °C
79 until the weight changed of less than 0.0005 g using analytical balance with an accuracy
80 ±0.0001 g. In order to prevent the mould growth, 0.5 g of thymol was placed in desiccators
81 with relative humidity > 60% (*a_w* > 0.60). The moisture content was determinate by AOAC
82 Official Method 930.04 (AOAC, 2007). Three replicates of equilibrium moisture contents at
83 each *a_w* level were used.

84

85 2.5 Isotherm modelling

86 Equilibrium moisture content was plotted as a function of water activity using the GAB
87 equation for both unroasted and roasted carob powder samples. The GAB equation was used
88 in the form:

89

$$90 \quad M = \frac{M_0 C K a_w}{[(1 - K a_w)(1 - K a_w + C K a_w)]} \quad (1)$$

91

92 where *M₀* (g g⁻¹ db) is monolayer moisture content and *C* and *K* represent parameters.

93

94 2.6 Thermodynamic properties of moisture sorption

95 Net isosteric heat, *q_{st}* (kJ mol⁻¹) was obtained from Claussius-Clapeyron equation:

$$96 \quad q_{st} = -R \frac{d \ln a_w}{d(1/T)} \quad (2)$$

97

98 where *T* is the temperature (K) and *R* is the universal gas constant (8.314 J (mol K)⁻¹). Net

99 isosteric heat is the important parameter describing the energy requirements for drying and the

100 state of water molecules in dried products. The relationship between q_{st} and differential
101 entropy of sorption (S_d , kJ (mol K)⁻¹) is described by the equation:

102

$$103 \quad (\ln a_w)_M = -\frac{q_{st}}{RT} + \frac{S_d}{T} \quad (3)$$

104 Net isosteric heat and differential entropy were obtained from the slope and intercept of the
105 fitted line $\ln(a_w)$ vs. $1/T$ at the constant moisture content (M), respectively.

106

107 2.7 Compensation theory

108 Linear relationship between q_{st} and S_d is the main assumption of applying the enthalpy-
109 entropy compensation theory (McMinn, Al-Muhtaseb, & Magee, 2005), i.e.:

110

$$111 \quad q_{st} = T_\beta S_d + \Delta G \quad (4)$$

112

113 where isokinetic temperature (T_β) and the change of the free energy (ΔG) were calculated
114 using linear regression. At isokinetic temperature, all the reactions occurred at the same rate
115 during sorption process. If $T_\beta \neq T_{hm}$ (harmonic temperature), the compensation theory is valid.

116 Harmonic temperature was defined in the form (Krug, Hunter, & Grieger, 1976):

117

$$118 \quad T_{hm} = \frac{n}{\sum_1^n (1/T)} \quad (5)$$

119

120 where n is the number of isotherms.

121

122 2.8 Integral enthalpy and entropy

123 Total energy required for binding the water molecules to the solid is described by the net
 124 integral enthalpy (q_{int}). It is similarly calculated as differential enthalpy (i.e. isosteric heat) but
 125 at constant spreading pressure ϕ

$$126 \quad q_{eq} = -R \left[\frac{d(\ln a_w)}{d(1/T)} \right]_{\phi} \quad (6)$$

127
 128 After plotting $\ln(a_w)$ against $1/T$ at constant spreading pressure using linear regression
 129 technique, the slope of the curve was used to estimate net integral enthalpy. The variation of
 130 net integral enthalpy with moisture content shows whether the interactions of water/solid are
 131 greater than those among water molecules (Vigano et al., 2012).

132 The difference between energy of liquid and solid phases can be described by spreading
 133 pressure, which corresponds to the lowering of surface tension of the liquid during adsorption.
 134 In this study, the spreading pressure was estimated using a procedure described in Kaya &
 135 Kahyaoglu (2006) from the equation:

$$136 \quad \phi = \frac{K_B T}{A_m} \int_0^{a_w} \frac{M}{M_0 a_w} d(a_w) \quad (7)$$

137
 138 where K_B is the Boltzmann constant ($1.38 \times 10^{-23} \text{ J K}^{-1}$), T is temperature (K), A_m is the area of
 139 the water molecule ($1.06 \times 10^{-19} \text{ m}^2$), M is the equilibrium moisture content, and M_0 is the
 140 monolayer moisture content. When substituting GAB equation (Eq. 1) to the Eq. (7), the
 141 following equation was obtained for the calculation of spreading pressure (Lago, Liendo-
 142 Cardenas, & Norena, 2013):

$$143 \quad \phi = \frac{K_B T}{A_m} \ln \left[\frac{1 + CKa_w - Ka_w}{1 - ka_w} \right]_{0.05}^{a_w} \quad (8)$$

146

147 The randomness of motion of water molecules is described by the net integral entropy (S_{int})

148 using the equation:

149

$$150 \quad S_{int} = -\frac{q_{int}}{T} - R \ln(a_w) * \quad (9)$$

151 where $(a_w)^*$ is the geometric mean water activity obtained at the constant spreading pressure

152 at different temperatures (Torres, Moreira, Chenlo, & Vazquez, 2012).

153

154 2.9 Differential scanning calorimetry and modelling of the glass transition curves

155 The glass transition temperatures of roasted and unroasted carob samples at different moisture

156 contents were measured by differential scanning calorimeter DSC 204F1 Phoenix (Netzsch,

157 Germany). Prior to analyses, calorimeter was calibrated by using a multipoint method (Hg, In,

158 Sn, Bi, Zn and CsCl). Samples (8–10 mg) were sealed in aluminium pans and an empty pan

159 was used as reference, while liquid nitrogen was used for sample cooling before runs.

160 Thermal program consisted in a two cycle-scan model with the temperature ranging from - 80

161 to 200 °C at a rate of 10 °C min⁻¹. All analyses were taken in two independent scans.

162 Obtained thermograms were analysed using NETZSCH *Proteus*® thermal analysis software

163 (Netzsch, Germany). The glass transition temperature (T_g) was taken as the midpoint of the

164 baseline shift in the second scan. The plasticizing effect of water on the glass transition

165 temperature was described by the following Gordon-Taylor model:

$$166 \quad T_g = \frac{T_{gs}X_s + kT_{gw}X_w}{X_s + kX_w} \quad (10)$$

167 where T_g is experimental glass transition temperature (°C), T_{gs} is glass transition temperature

168 for anhydrous solid (°C), T_{gw} is glass transition temperature of pure water (°C), X_s is a mass

169 fraction of the solute, X_w is a mass fraction of water and k is a constant depending on the

170 system respectively. Glass transition temperature of pure water was taken as $-135\text{ }^{\circ}\text{C}$
171 (Moraga, Talens, Moraga, & Martinez-Navarrete, 2011).

172

173 2.10 Statistical analysis

174 The parameters of GAB isotherms and Gordon-Taylor equation were evaluated using non-
175 linear regression analysis (OriginPro v. 5.0, OriginLab Corp., Northampton, MA, USA) using
176 Revenberg-Marquardt iteration algorithm until minimal values of the residual sum of squares
177 (RSS) were obtained. The goodness of fit of the experimental data was evaluated by the
178 coefficient of determination (r^2), and by the mean relative percentage deviation (E , %)
179 between experimental (M_{exp}) and predicted values (M_{pred}) moisture content using the formula

180

$$181 \quad E = \frac{100}{n} \sum_{i=1}^N \frac{|M_{exp} - M_{pred}|}{M_{exp}} \quad (11)$$

182

183 The model is acceptable if E value is below 10%. Statistical differences were evaluated using
184 One-way analysis of variance (ANOVA). All the statistical treatments of the data were
185 performed at the probability level $p = 0.05$.

186

187 3. Results and discussion

188 3.1 Proximate composition of carob powder samples

189 The main composition of both unroasted and roasted carob powder is presented in Suppl. 1.

190 As can be seen, roasting at $130\text{ }^{\circ}\text{C}$ for 30 min did not influence the content of crude protein,

191 crude fat and total dietary fibre. Reducing sugars decreased from 13.12. to 12.51 % after

192 thermal treatment ($p>0.05$) and the small but significant increase in ash content from 3.29 to

193 3.70 % has been observed ($p<0.05$). The both decrease in sugar content and increase in ash

194 content were similar to roasting of carob pod powder in temperatures ranged from 110 °C to
195 150 °C, probably due to the involvement in Maillard reaction (Boublenza et al., 2017).

196

197 3.2 Moisture adsorption isotherms

198 Equilibrium moisture content of carob powder was plotted against water activity and
199 isotherms were constructed by applying GAB equation (Eq. 1) via non-linear regression (Fig.
200 1). The estimated parameters of the GAB isotherm are presented in Table 1. together with
201 high value of r^2 (0.990–0.997) and low mean relative percentage deviations E (5.76–8.91 %)
202 for both samples at all the temperatures.

203 As can be seen from Fig. 1, equilibrium moisture content is increasing with the increase of
204 water activity for both samples. The type II isotherms (sigmoid shape) were observed for
205 carob powders according to the BET classification (Brunauer, Emmett, & Teller, 1938).

206 Significantly higher moisture content at 15 °C was determined for unroasted carob powder in
207 the whole water activity range ($p < 0.05$), while isotherms for 25 °C and 40 °C were almost
208 identical ($p > 0.05$). Roasted carob powder exhibited similar EMC up to 0.43 a_w for all the
209 temperatures followed by significantly higher EMC for isotherm at 15 °C in the range from
210 0.43 to 0.90 a_w ($p < 0.05$). The latter is caused by the exothermic character of sorption process
211 as was confirmed for other food products (Moreira, Chenlo, Torres, & Prieto, 2010;

212 Baptestini, Correa, de Oliveira, Cecon, & Soares, 2017; Polatoglu, Bese, Kaya, & Aktas,

213 2011). Roasted carob powder adsorbed less moisture than unroasted counterparts at all the

214 temperatures probably due to the structural and chemical changes initiated by the high

215 temperature during roasting process. The interactions between the carbohydrates and proteins
216 or the increase of protein hydrophobicity may occur during temperature treatment. It follows

217 the limited number of sorption sites capable to adsorb molecules as found for Argentinean

218 Algarobba pods (Prokopiuk, Martinez-Navarrete, Andres, Chiralt, & Cruz, 2010), Yerba mate

219 leaves (Cervenka, Hlouskova, & Zabcikova, 2015) and coffee (Rocculi et al., 2011).
220 However, higher EMC values above $\sim 0.70 a_w$ at 15 °C were observed for roasted carob
221 powder in agreement with the study of Rocculi et al. (2011). The upper part of isotherm
222 corresponds to the adsorption of bulk water into the large pores of solid causing swelling and
223 solute dissolution. It may suggest that roasting process increase the number of pores (or their
224 volumes), hence the equal volume of water resulted in higher adsorption. However, several
225 authors subjected moisture adsorption and particle size distribution to examination and found
226 that there is no significant relationship (Baptestini, Correa, de Oliveira, Cecon, & Soares,
227 2017; de Oliveira, Correa, de Oliveira, Baptestini, & Vargas-Elias, 2017). They found the
228 differences in moisture sorption characteristics among coffee samples with various degree of
229 roasting but did not find correlation with particle size. Therefore, some chemical modification
230 could be also responsible for higher moisture adsorption of roasted carob powder at high
231 water activities.

232 Monolayer moisture is the important parameter defining moisture strongly adsorbed to the
233 surface of the food matrix. The monolayer values were estimated to $0.065\text{--}0.082 \text{ g g}^{-1} \text{ db}$ and
234 $0.047\text{--}0.063 \text{ g g}^{-1} \text{ db}$ for unroasted and roasted carob powder, respectively. These values were
235 close to monolayer values of wheat and chestnut flour (Moreira, Chenlo, Torres, & Prieto,
236 2010), prosopis pod (Prokopiuk, Martinez-Navarrete, Andres, Chiralt, & Cruz, 2010) and
237 chironji kernels (Sahu et al., 2018). As can be seen from Table 2, monolayer values for
238 roasted carob samples were significantly lower in comparison with unroasted carob samples
239 at the same temperature similarly to our previous study (Cervenka, Hlouskova, & Zabcikova,
240 2015).

241

242 3.3 Differential thermodynamic properties of moisture adsorption

243 The net isosteric heat of adsorption was calculated according the Eq. (2) and plotted against
244 moisture content (Fig. 2). The curves showed that the net isosteric heat decreased with the
245 increase of EMC as was described in foods (McMinn, McKee, Ronald, & Magee, 2007;
246 Moreira, Chenlo, Torres, & Prieto, 2010). At low moisture content, surface of the solid
247 exposed active sites strongly bound the water molecules and formed mono-molecular layer.
248 Once these highly-energy active sites are occupied, the lower-energy active sites are exposed
249 with the increase of moisture content (McMinn, McKee, Ronald, & Magee, 2007). At
250 particular EMC point, the heat of sorption remained stable indicating the multilayer
251 adsorption process. Unroasted carob powder exhibited higher net isosteric heat of adsorption
252 then that of roasted carob powder in the range of moisture content from 0.08 to 0.12 g g⁻¹ db
253 (Fig. 2A). Net isosteric heat of adsorption for unroasted carob powder was 24.9 kJ mol⁻¹ at
254 0.08 g g⁻¹ db followed by sharp decline to 10.1 kJ mol⁻¹ at 0.10 g g⁻¹ db, while small decrease
255 from 6.8 to 6.2 kJ mol⁻¹ was obtained for roasted carob powder with the increase of moisture
256 content from 0.08 to 0.10 g g⁻¹ db. Above particular moisture content (i.e. 0.12 g g⁻¹ db),
257 roasted carob powder showed lower net isosteric heat of adsorption (2.0 kJ mol⁻¹) than that
258 for unroasted counterparts (4.8 kJ mol⁻¹). It corresponds with our previous findings for green
259 and roasted Yerba mate leaves (Cervenka, Hlouskova, & Zabcikova, 2015). Fig. 2B shows the
260 effect of moisture content on differential entropy, S_d , calculated from Eq. (3). Differential
261 entropy for both carob samples increased with the increase of moisture content similarly to
262 medium-light roasted coffee in a study of de Oliveira et al. (2017). They explained the
263 increase in S_d by the formation of water molecule layers during adsorption process. At high
264 equilibrium moisture content, the active sites are saturated and S_d values approaches to zero
265 (differential entropy of pure water).

266

267 3.4 Compensation theory

268 The values of net isosteric heat of sorption was linearly dependent on differential entropy
269 values for both carob powder samples as shown in Suppl. 2. Therefore, the enthalpy-entropy
270 compensation theory is valid and can be described by the equations $q_{st} = 357.1 S_d + 0.41$ ($r^2 =$
271 0.999) and $q_{st} = 518.5 S_d - 1.77$ ($r^2 = 0.998$) for unroasted and roasted carob powder,
272 respectively. The harmonic mean temperature (T_{hm}) was calculated from the Eq. (5) and found
273 as 299.6 K. The isokinetic temperatures T_β were (357.1 ± 1.1) K and (518.5 ± 7.9) K for
274 unroasted and roasted carob powders, respectively. Since the condition $T_{hm} < T_\beta$ was
275 confirmed, the adsorption process is enthalpy-driven. In addition, positive free Gibbs energy
276 for unroasted carob powder ($\Delta G = 0.41 \text{ kJ mol}^{-1}$) indicates nonspontaneous adsorption
277 process while spontaneity was evident for roasted powder ($\Delta G = -1.80 \text{ kJ mol}^{-1}$) in the whole
278 range of EMC. Enthalpy-driven and nonspontaneous adsorption process was determined in
279 oatmeal biscuit and flakes (McMinn, McKee, Ronald, & Magee, 2007) or Yerba mate leaves
280 (Cervenka, Hlouskova, & Zabcikova, 2015), while the spontaneity of adsorption was
281 observed for Turkish fermented sausage (Polatoglu, Bese, Kaya, & Aktas, 2011).

282

283 3.5 Spreading pressure and integral thermodynamic of adsorption

284 The spreading pressure for both carob powder samples was calculated according to Eq. (7)
285 and its variation with water activity is presented in Suppl. 3. The values of ϕ increased with
286 the increase of a_w and decreased with the increase of temperature as was found in other foods
287 (Polatoglu, Bese, Kaya, & Aktas, 2011; Kaya & Kahyaoglu, 2006). Spreading pressure
288 represents the free energy at the surface of sorption sites of the solid and its high values
289 indicates higher affinity of water molecules to active sites. Unroasted carob powder has lower
290 spreading pressure at a given a_w values in comparison with roasted carob powder in the whole
291 water activity range. Similar conclusions were observed when examining unroasted and
292 roasted dehulled sesame seed (Kaya & Kahyaoglu, 2006).

293 The net integral enthalpy (q_{int}) was calculated using Eq. (9), by plotting $\ln(a_w)$ against $1/T$ for
294 a specific spreading pressure. In Fig. 3, the net integral enthalpy of adsorption of carob
295 powders was plotted as a function of moisture content. For unroasted carob powder, the
296 enthalpy increases until maximum value of $24.37 \text{ kJ mol}^{-1}$ at moisture content of $0.12 \text{ g g}^{-1} \text{ db}$
297 followed by gradual decrease with further increase in moisture content (Fig. 3A). At low
298 moisture content, water is adsorbed on the most accessible sites on surface of carob powder
299 causing swelling of material. The swelling is responsible for opening of new high energy
300 locations where new water binding can be developed. At higher moisture content (above 0.12
301 $\text{g g}^{-1} \text{ db}$), high-energy binding sites are occupied by water molecules remaining less
302 favourable locations to be covered with them. Therefore, net integral enthalpy decreased with
303 the increase of moisture content. This behaviour was also observed in brown seaweed
304 (Moreira, Chenlo, Sineiro, Sanchez, & Arufe, 2016) or Swiss cheese microparticles (Silva,
305 Borges, da Costa, & Queiroz, 2015). On the other hand, enthalpy variation with moisture
306 content for roasted carob powder showed different pattern. A steep decline from maximum
307 value of $27.15 \text{ kJ mol}^{-1}$ to $11.24 \text{ kJ mol}^{-1}$ was observed at low moisture content in the range
308 from 0.03 to $0.06 \text{ g g}^{-1} \text{ db}$ (Fig. 3A). This trend was also observed in oatmeal biscuits
309 (McMinn, McKee, Ronald, & Magee, 2007). Increasing trend of net integral enthalpy at low
310 moisture content indicates the greater water-solid interactions compared to the interactions of
311 water molecules (Kaya & Kahyaoglu, 2006).

312 The net integral entropy was calculated using the same Eq. (9) but from the intercept value.
313 Initially, the entropy was observed to decrease with the increase of moisture content from
314 0.04 to $0.12 \text{ g g}^{-1} \text{ db}$ for unroasted carob powder (Fig. 3B). It ranges from -16.34 to -73.75 kJ
315 $(\text{mol K})^{-1}$. In very low EMC, water molecules are initially bonded to highly-active sites in
316 solid surface keeping certain degree of movements. While those readily available sites are
317 occupied, additional water molecules attached to less favourable active sites followed by their

318 further localization. When water molecules covered all the active sites on the surface, the
319 minimum of integral entropy was achieved forming the first layer. Further increase of net
320 integral enthalpy with the increase of EMC is due to the formation of multilayer. Regarding
321 roasted carob powder, net integral entropy decreased from $-67.34 \text{ kJ (mol K)}^{-1}$ to -27.19 kJ
322 $(\text{mol K})^{-1}$ in EMC ranged from 0.03 to 0.06 g g^{-1} db. For both samples, net integral entropy
323 tends to reach the entropy of free water. Based on the results, we may assume that roasting
324 process changed the surface of the sample by exposing all the hidden high energy locations to
325 the direct interaction with water molecules (without swelling of material). This statement was
326 also supported by similar maximal and minimal values of net integral enthalpy and entropy,
327 respectively, for unroasted and roasted carob powder.

328

329 3.6 Glass transition temperature

330 Values of T_g obtained for roasted and unroasted carob samples as a function of equilibrium
331 moisture content are shown in Suppl. 4. As expected for both materials T_g values decreased as
332 equilibrium moisture content (or water activity) increased. It can be related with the
333 plasticizing effect of the water, contributing to the storage and stability of the foodstuff. Water
334 acts as a plasticizer by reducing the T_g due to reduction of the inter- and intra-macromolecular
335 forces (Shi, Lin, Zhao, & Zhang, 2015). The similar trend was observed in our previous study
336 for burdock and elecampe roots (Cervenka, Kubinova, Juszczak, & Witczak, 2012).
337 Experimental data of T_g varied from -45.0 to $62.6 \text{ }^\circ\text{C}$ for unroasted samples and from -38.3
338 to $67.9 \text{ }^\circ\text{C}$ for roasted material. The roasted carob powder showed higher glass transition
339 temperatures as compared to unroasted material, which is related with higher hygroscopicity
340 of unroasted sample. For example, equilibrium moisture content of unroasted carob at $0.23 a_w$
341 is 0.044 g g^{-1} db while 0.028 g g^{-1} db for roasted carob powder at $25 \text{ }^\circ\text{C}$. The lower T_g values
342 obtained for unroasted material can be also related to the higher concentration of reducing

343 sugar content (see Suppl. 1), although not statistically significant ($p > 0.05$). It is known that
344 low molecular weight compounds such as simple sugars or organic acid reduced glass
345 transition temperature (Roos, Karel, & Kokini, 1996). Moreover, the higher value of T_g
346 obtained for roasted material may be results of changes like a Maillard reaction occurring
347 during roasting process. Differences in the thermal properties before and after roasting
348 process were observed for coffee beans (Rivera et al., 2011). The experimental data of T_g
349 fitted well to the Gordon-Taylor model showing high values of r^2 (above 0.980). The
350 parameters obtained from the model are presented in Table 2. Values of the constant T_{gs} ,
351 corresponding to glass transition of anhydrous material were 61.8 and 65.7 °C for unroasted
352 and roasted carob powder, respectively. The predicted values of T_g are similar to the
353 previously reported values obtained for other materials with high level of dietary fibre such as
354 date flesh (Rahman, 2004) or freeze-dried pineapple (Telis & Sobral, 2001). Higher T_g values
355 obtained for unroasted material confirm that it may contains less low molecular weight
356 components than unroasted sample. The k parameter controls degree of curvature of T_g
357 dependence on water content in a binary system and can be related with the strength of
358 interaction between water and foods solids. Higher value of k indicate a greater plasticizing
359 effect of water on solids (Shi, Lin, Zhao, & Zhang, 2015). The calculated values of k for
360 roasted and unroasted carob were 6.05 and 5.68, respectively. These values may indicate that
361 plasticizing effect of water was more significant in the roasted material than in unroasted one.

362

363 3.7 Critical conditions of storage

364 When combining the glass transition temperature concept with sorption isotherms, one can
365 obtain a useful tool for estimation of critical values for a_w and moisture content. For
366 estimation of the critical moisture content in carob powder samples, the adsorption isotherms
367 using GAB equation at 25 °C and the plots of T_g vs. a_w were constructed (Fig. 4A-B).

368 Applying this concept, critical water activity and critical moisture content for the glass
369 transition of unroasted and roasted carob powders were 0.38 a_w (corresponded to 0.077 g g⁻¹
370 db) and 0.43 a_w (corresponded to 0.058 g g⁻¹ db), respectively. It seems that roasted carob
371 powder can be considered as most stable since it showed higher critical water activity. The
372 glassy state of the product would be ensured up to 0.43 a_w upon storing.

373

374 4. Conclusion

375 To the best of our knowledge, this study represents the first report describing the moisture
376 adsorption characteristics of carob powder (*Ceratonia siliqua* L.). Since thermally treated
377 carob powder/flour is also available in the market, two types (unroasted and roasted) of carob
378 powders were used to elucidate the differences in thermodynamic properties of moisture
379 adsorption. The isotherms were evaluated at temperature range of 15–40 °C and were of type
380 II commonly observed in the most foods. The GAB model was found to be suitable for
381 adsorption of both carob powder samples. At 15 °C, unroasted carob powder was susceptible
382 to adsorb more moisture in the whole a_w range, while roasted carob powder was more
383 hygroscopic above 0.43 a_w at the same temperature. Moisture adsorption was similar at 25 °C
384 and 40 °C for both carob samples. Both the net isosteric heat and differential entropy
385 decreased with the increase in moisture content showing that the adsorbed water molecules
386 are strongly bound to the surface at low moisture content for unroasted carob powder in
387 comparison with that of roasted carob powder. Enthalpy-entropy compensation theory was
388 successfully applied and suggests that the adsorption process is enthalpy driven. The study of
389 integral thermodynamic properties of adsorption process for carob powder samples revealed
390 particular differences, i.e. maximal and minimal values for net integral enthalpy and entropy,
391 respectively, were observed for unroasted carob powder. It means that probably swelling of
392 the material occurred during the adsorption process. The glass transition was determined in

393 0.077 and 0.058 g of moisture per gram of dry basis for unroasted and roasted carob powder,
394 respectively. The combination of Gordon-Taylor and GAB models into one plot revealed that
395 roasting of carob powder at 130 °C for 30 min made this product more stable for storage
396 purposes. Therefore, we may conclude that the hypothesis was confirmed. In addition, further
397 investigations of chemical stability (polyphenols, fat) at different storage conditions are
398 needed.

399

400 Conflict of interests

401 The authors have declared no conflict of interest

402

403 Acknowledgement

404 The projects SGS_2019_003 of University of Pardubice and BM-2705/KIAPS/2018 of
405 University of Agriculture are gratefully acknowledged.

406

407 References

408 Al-Muhtaseb, A. H., McMinn, W. A. M., & Magee, T. R. A. (2002). Moisture sorption
409 isotherm characteristics of food products: A review. *Food and Bioproducts*
410 *Processing*, 80(C2), 118-128. doi: Doi 10.1205/09603080252938753

411 Ayaz, F. A., Torun, H., Glew, R. H., Bak, Z. D., Chuang, L. T., Presley, J. M., & Andrews, R.
412 (2009). Nutrient content of carob pod (*Ceratonia siliqua* L.) flour prepared
413 commercially and domestically. *Plant Foods for Human Nutrition*, 64(4), 286-292.
414 doi: 10.1007/s11130-009-0130-3

415 Baptestini, F. M., Correa, P. C., de Oliveira, G. H. H., Cecon, P. R., & Soares, N. D. F.
416 (2017). Kinetic modeling of water sorption by roasted and ground coffee. *Acta*
417 *Scientiarum-Agronomy*, 39(3), 273-281. doi: 10.4025/actasciagron.v39i3.32576

418 Biernacka, B., Dziki, D., Gawlik-Dziki, U., Rozylo, R., & Siastala, M. (2017). Physical,
419 sensorial, and antioxidant properties of common wheat pasta enriched with carob
420 fiber. *Lwt-Food Science and Technology*, 77, 186-192. doi: 10.1016/j.lwt.2016.11.042

421 Boublenza, I., Lazouni, H. A., Ghaffari, L., Ruiz, K., Fabiano-Tixier, A. S., & Chemat, F.
422 (2017). Influence of roasting on sensory, antioxidant, aromas, and physicochemical
423 properties of carob pod powder (*Ceratonia siliqua* L.). *Journal of Food Quality*. doi:
424 Artn 4193672
425 10.1155/2017/4193672

426 Brunauer, S., Emmett, P. H., & Teller, E. (1938). Adsorption of gases in multi-molecular
427 layers. *Journal of American Chemical Society*, 62, 309-309.

428 Cepo, D. V., Mornar, A., Nigovic, B., Kremer, D., Radanovic, D., & Dragojevic, I. V. (2014).
429 Optimization of roasting conditions as an useful approach for increasing antioxidant
430 activity of carob powder. *Lwt-Food Science and Technology*, 58(2), 578-586. doi:
431 10.1016/j.lwt.2014.04.004

432 Cervenka, L., Hlouskova, L., & Zabcikova, S. (2015). Moisture adsorption isotherms and
433 thermodynamic properties of green and roasted Yerba mate (*Ilex paraguariensis*).
434 *Food Bioscience*, 12, 122-127. doi: 10.1016/j.fbio.2015.10.001

435 Cervenka, L., Kubinova, J., Juszczak, L., & Witczak, M. (2012). Moisture sorption isotherms
436 and glass transition temperature of elecampe (*Inula helenium* L.) and burdock
437 (*Arctium lappa* L.) roots at 25 degrees C. *Food Science and Technology International*,
438 18(1), 81-91. doi: 10.1177/1082013211414260

439 de Oliveira, G. H. H., Correa, P. C., de Oliveira, A. P. L. R., Baptestini, F. M., & Vargas-
440 Elias, G. A. (2017). Roasting, grinding, and storage impact on thermodynamic
441 properties and adsorption isotherms of Arabica coffee. *Journal of Food Processing*
442 *and Preservation*, 41(2). doi: ARTN e12779
443 10.1111/jfpp.12779

444 Greenspan, L. (1977). Humidity fixed-points of binary saturated aqueous-solutions. *Journal*
445 *of Research of the National Bureau of Standards Section a-Physics and Chemistry*,
446 *81(1)*, 89-96. doi: 10.6028/jres.081A.011

447 Kaya, S., & Kahyaoglu, T. (2006). Influence of dehulling and roasting process on the
448 thermodynamics of moisture adsorption in sesame seed. *Journal of Food Engineering*,
449 *76(2)*, 139-147. doi: 10.1016/f.foodeng.2005.04.042

450 Krug, R. R., Hunter, W. G., & Grieger, R. A. (1976). Enthalpy-entropy compensation .1.
451 Some fundamental statistical problems associated with analysis of Vant Hoff and
452 Arrhenius data. *Journal of Physical Chemistry*, *80(21)*, 2335-2341. doi: Doi
453 10.1021/J100562a006

454 Lago, C. C., Liendo-Cardenas, M., & Norena, C. P. Z. (2013). Thermodynamic sorption
455 properties of potato and sweet potato flakes. *Food and Bioproducts Processing*,
456 *91(C4)*, 389-395. doi: 10.1016/j.fbp.2013.02.005

457 Loullis, A., & Pinakoulaki, E. (2018). Carob as cocoa substitute: a review on composition,
458 health benefits and food applications. *European Food Research and Technology*,
459 *244(6)*, 959-977. doi: 10.1007/s00217-017-3018-8

460 McMinn, W. A. M., Al-Muhtaseb, A. H., & Magee, T. R. A. (2005). Enthalpy-entropy
461 compensation in sorption phenomena of starch materials. *Food Research*
462 *International*, *38(5)*, 505-510. doi: 10.1016/j.foodres.2004.11.004

463 McMinn, W. A. M., McKee, D. J., Ronald, T., & Magee, A. (2007). Moisture adsorption
464 behaviour of oatmeal biscuit and oat flakes. *Journal of Food Engineering*, *79(2)*, 481-
465 493. doi: 10.1016/j.jfoodeng.2006.02.009

466 Moraga, G., Talens, P., Moraga, M. J., & Martinez-Navarrete, N. (2011). Implication of water
467 activity and glass transition on the mechanical and optical properties of freeze-dried

468 apple and banana slices. *Journal of Food Engineering*, 106(3), 212-219. doi:
469 10.1016/j.jfoodeng.2011.05.009

470 Moreira, R., Chenlo, F., Sineiro, J., Sanchez, M., & Arufe, S. (2016). Water sorption
471 isotherms and air drying kinetics modelling of the brown seaweed *Bifurcaria*
472 *bifurcata*. *Journal of Applied Phycology*, 28(1), 609-618. doi: 10.1007/s10811-015-
473 0553-1

474 Moreira, R., Chenlo, F., Torres, M. D., & Prieto, D. M. (2010). Water adsorption and
475 desorption isotherms of chestnut and wheat flours. *Industrial Crops and Products*,
476 32(3), 252-257. doi: 10.1016/j.indcrop.2010.04.021

477 Mosquera, L. H., Moraga, G., & Martinez-Navarrete, N. (2012). Critical water activity and
478 critical water content of freeze-dried strawberry powder as affected by maltodextrin
479 and arabic gum. *Food Research International*, 47(2), 201-206. doi:
480 10.1016/j.foodres.2011.05.019

481 Polatoglu, B., Bese, A. V., Kaya, M., & Aktas, N. (2011). Moisture adsorption isotherms and
482 thermodynamics properties of sucuk (Turkish dry-fermented sausage). *Food and*
483 *Bioproducts Processing*, 89(C4), 449-456. doi: 10.1016/j.fbp.2010.06.003

484 Prokopiuk, D., Martinez-Navarrete, N., Andres, A., Chiralt, A., & Cruz, G. (2010). Influence
485 of roasting on the water sorption isotherms of Argentinean Algarroba (*Prosopis alba*
486 *Griseb*) pods. *International Journal of Food Properties*, 13(4), 692-701. doi:
487 10.1080/10942910902742055

488 Rahman, M. S. (2004). State diagram of date flesh using Differential Scanning Calorimetry
489 (DSC). *International Journal of Food Properties*, 7(3), 407-428. doi: 10.1081/Jfp-
490 120030050

- 491 Rahman, M. S. (2006). State diagram of foods: Its potential use in food processing and
492 product stability. *Trends in Food Science & Technology*, 17(3), 129-141. doi:
493 10.1016/tifs.2005.09.009
- 494 Rivera, W., Velasco, X., Galvez, C., Rincon, C., Rosales, A., & Arango, P. (2011). Effect of
495 the roasting process on glass transition and phase transition of Colombian Arabic
496 coffee beans. *11th International Congress on Engineering and Food (Icef11)*, 1, 385-
497 390. doi: 10.1016/j.profoo.2011.09.059
- 498 Rocculi, P., Sacchetti, G., Venturi, L., Cremonini, M., Rosa, M. D., & Pittia, P. (2011). Role
499 of water state and mobility on the antiplasticization of green and roasted coffee beans.
500 *Journal of Agricultural and Food Chemistry*, 59(15), 8265-8271. doi:
501 10.1021/jf201333a
- 502 Roos, Y. H., Karel, M., & Kokini, J. L. (1996). Glass transitions in low-moisture and frozen
503 foods: Effects on shelf life and quality. *Food Technology*, 50(11), 95-108.
- 504 Rtibi, K., Selmi, S., Grami, D., Amri, M., Eto, B., El-Benna, J., . . . Marzouki, L. (2017).
505 Chemical constituents and pharmacological actions of carob pods and leaves
506 (*Ceratonia siliqua* L.) on the gastrointestinal tract: A review. *Biomedicine &*
507 *Pharmacotherapy*, 93, 522-528. doi: 10.1016/j.biopha.2017.06.088
- 508 Sahu, S. N., Tiwari, A., Sahu, J. K., Naik, S. N., Baitharu, I., & Kariali, E. (2018). Moisture
509 sorption isotherms and thermodynamic properties of sorbed water of chironji
510 (*Buchanania lanzan* Spreng.) kernels at different storage conditions. *Journal of Food*
511 *Measurement and Characterization*, 12(4), 2626-2635. doi: 10.1007/s11694-018-
512 9880-7
- 513 Shi, Q. L., Lin, W. W., Zhao, Y., & Zhang, P. P. (2015). Thermal characteristics and state
514 diagram of *Penaeus vannamei* meat with and without maltodextrin addition.
515 *Thermochimica Acta*, 616, 92-99. doi: 10.1016/j.tca.2015.08.016

516 Silva, E. K., Borges, S. V., da Costa, J. M. G., & Queiroz, F. (2015). Thermodynamic
517 properties, kinetics and adsorption mechanisms of Swiss cheese bioaroma powder.
518 *Powder Technology*, 272, 181-188. doi: 10.1016/j.powtec.2014.12.002

519 Telis, V. R. N., & Sobral, P. J. A. (2001). Glass transitions and state diagram for freeze-dried
520 pineapple. *Lebensmittel-Wissenschaft Und-Technologie-Food Science and*
521 *Technology*, 34(4), 199-205. doi: 10.1006/fstl.2000.0685

522 Tonon, R. V., Baroni, A. F., Brabet, C., Gibert, O., Pallet, D., & Hubinger, M. D. (2009).
523 Water sorption and glass transition temperature of spray dried acai (*Euterpe oleracea*
524 Mart.) juice. *Journal of Food Engineering*, 94(3-4), 215-221. doi:
525 10.1016/j.jfoodeng.2009.03.009

526 Torres, M. D., Moreira, R., Chenlo, F., & Vazquez, M. J. (2012). Water adsorption isotherms
527 of carboxymethyl cellulose, guar, locust bean, tragacanth and xanthan gums.
528 *Carbohydrate Polymers*, 89(2), 592-598. doi: 10.1016/j.carbpol.2012.03.055

529 Turfani, V., Narducci, V., Durazzo, A., Galli, V., & Carcea, M. (2017). Technological,
530 nutritional and functional properties of wheat bread enriched with lentil or carob
531 flours. *Lwt-Food Science and Technology*, 78, 361-366. doi:
532 10.1016/j.lwt.2016.12.030

533 Vigano, J., Azuara, E., Telis, V. R. N., Beristain, C. I., Jimenez, M., & Telis-Romero, J.
534 (2012). Role of enthalpy and entropy in moisture sorption behavior of pineapple pulp
535 powder produced by different drying methods. *Thermochimica Acta*, 528, 63-71. doi:
536 10.1016/j.tca.2011.11.011

537
538
539

540 **Fig. 1** Equilibrium moisture content vs. water activity and moisture adsorption isotherms
541 fitted by GAB equation (continuous lines) of A) unroasted and B) roasted carob
542 powder at 15 °C (Δ), 25 °C (\square) and 40 °C (\circ). Vertical bars represent standard
543 deviation of replicates ($n=3$)

544

545 **Fig. 2** Net isosteric heat A) and differential entropy B) of unroasted (\square) and roasted (\circ) carob
546 powder adsorption vs. the moisture content

547

548 **Fig. 3** Integral enthalpy (A) and integral entropy (B) of unroasted (\blacksquare) and roasted (\circ) carob
549 powder adsorption vs. the moisture content.

550

551 **Fig. 4** Variation of glass transition temperature (T_g) and moisture content with water activity
552 for roasted (A) and unroasted (B) carob powders

556 Table 1 Regression parameters of GAB equation applied to moisture adsorption isotherms

Carob powder		Temperature (°C)		
		15	25	40
unroasted	M_0	0.078 ± 0.007	0.082 ± 0.016	0.065 ± 0.007
	C	8.790 ± 0.771	2.489 ± 0.317	2.801 ± 0.364
	K	0.994 ± 0.025	0.970 ± 0.033	1.007 ± 0.010
	r^2	0.996	0.990	0.996
	E (%)	7.59	7.20	8.91
roasted	M_0	0.063 ± 0.009	0.047 ± 0.003	0.062 ± 0.007
	C	4.770 ± 0.539	2.574 ± 0.543	1.536 ± 0.518
	K	1.085 ± 0.011	1.044 ± 0.006	1.000 ± 0.010
	r^2	0.990	0.994	0.997
	E (%)	7.24	5.76	8.37

557 An average ± standard deviation; M_0 , monolayer moisture content (g g^{-1} db); C and K ,
558 constant of GAB equation; r^2 , coefficient of determination; E , mean relative percentage
559 deviation (%)

560 Table 2 Nonlinear regression parameters of the Gordon-Taylor model for roasted and
561 unroasted carob

Parameter	Carob	
	unroasted	roasted
T_g (°C)	61.81	65.66
k	5.68	6.05
r^2	0.996	0.988

562

Fig. 1 Equilibrium moisture content vs. water activity and moisture adsorption isotherms fitted by GAB equation (continuous lines) of A) unroasted and B) roasted carob powder at 15 °C (Δ), 25 °C (\square) and 40 °C (\circ). Vertical bars represent standard deviation of replicates ($n=3$)

Fig. 2 Net isosteric heat A) and differential entropy B) of unroasted (\square) and roasted (\circ) carob powder adsorption vs the moisture content

Fig. 3 Integral enthalpy (A) and integral entropy (B) of unroasted (\blacksquare) and roasted (\circ) carob powder adsorption vs the moisture content.

Fig. 4 Variation of glass transition temperature (T_g) and moisture content with water activity for roasted (A) and unroasted (B) carob powders

Figure 1
[Click here to download high resolution image](#)

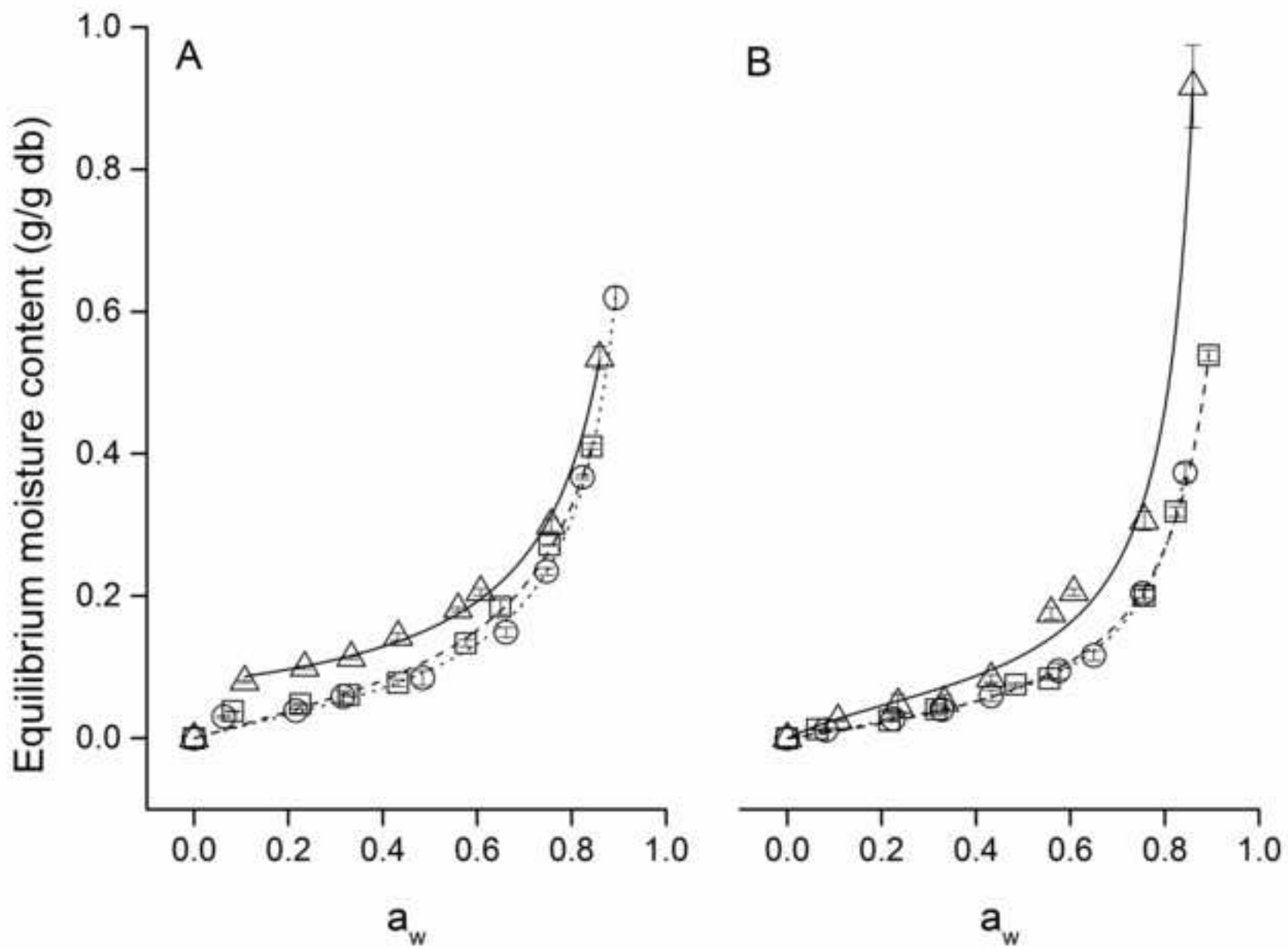


Figure 2
[Click here to download high resolution image](#)

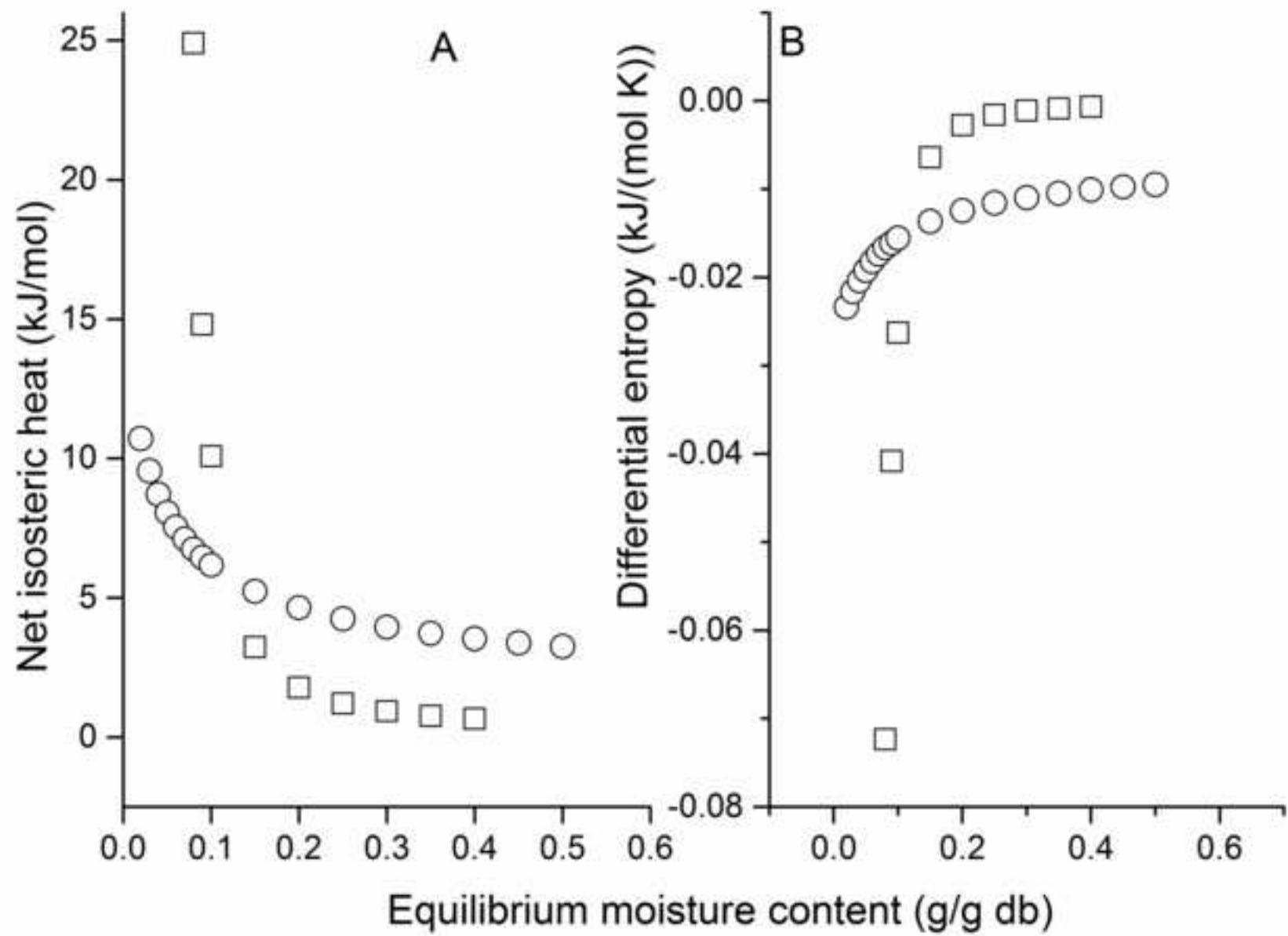


Figure 3
[Click here to download high resolution image](#)

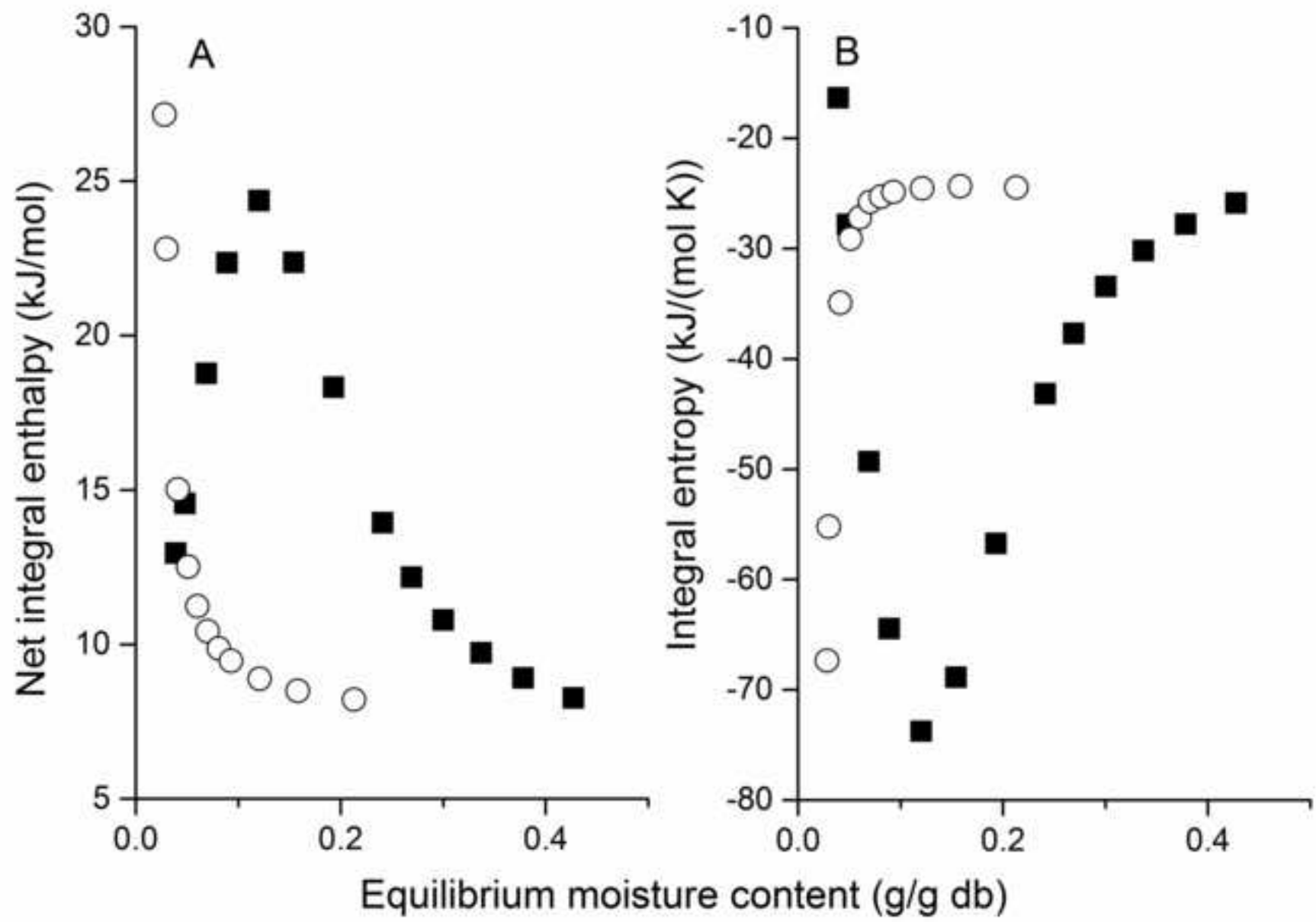
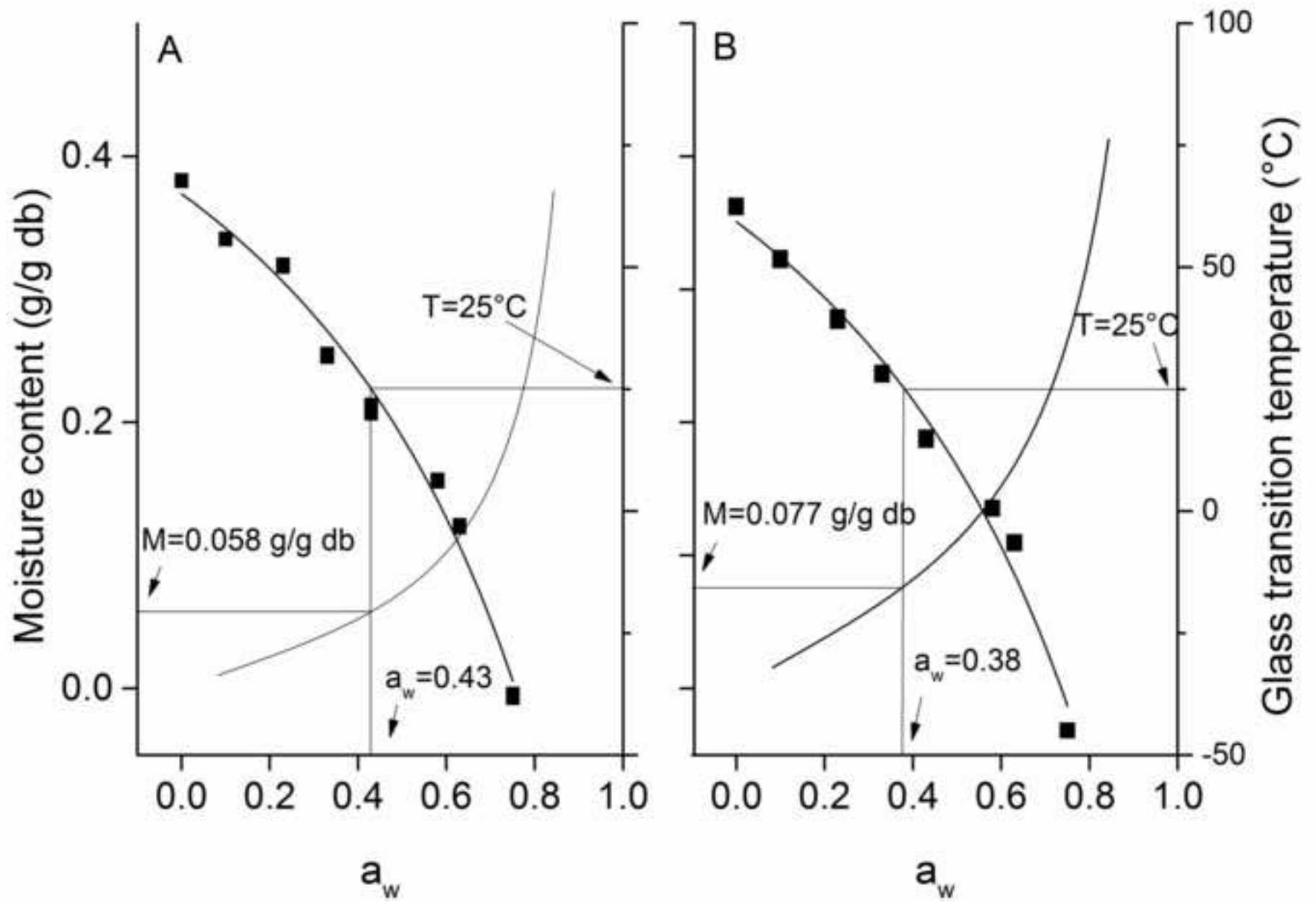


Figure 4
[Click here to download high resolution image](#)



Supplement 1 (Table)

[Click here to download Supplementary Material: Supplement 1.docx](#)

Supplement 3 (Table)

[Click here to download Supplementary Material: Supplement 3.docx](#)

Supplement captions

[Click here to download Supplementary Material: Supplement captions.docx](#)

Supplement 2 (Figure)

[Click here to download Supplementary Material: Supplement 2.tif](#)

Supplement 4 (Figure)

[Click here to download Supplementary Material: Supplement 4.tif](#)

Declaration of interests

The authors declare that they have no known competing financial interests or personal relationships that could have appeared to influence the work reported in this paper.

The authors declare the following financial interests/personal relationships which may be considered as potential competing interests:

Libor Červenka, in behalf of all authors

